Supplement of Atmos. Chem. Phys., 14, 11201–11219, 2014
http://www.atmos-chem-phys.net/14/11201/2014/
doi:10.5194/acp-14-11201-2014-supplement

Atmospheric Chemistry and Physics Open Access

Supplement of

Reactive bromine chemistry in Mount Etna's volcanic plume: the influence of total Br, high-temperature processing, aerosol loading and plume–air mixing

T. J. Roberts et al.

Correspondence to: T. J. Roberts (tjardaroberts@gmail.com)

S1 The high-temperature near-vent plume

The *PlumeChem* atmospheric chemistry model simulations of reactive halogen chemistry in the (ambient temperature) dispersing downwind plume are initialised with a representation of the high-temperature near-vent plume. Output from the commercially available (http://www.outotec.com/) Chemical Reaction and Equilibrium Software, HSC Chemistry, was used for this purpose, assuming a range of potential atmospheric:magmatic ratios (V_A:V_M) to calculate the input composition and temperature. Example data for V_A:V_M = 5:95 (T = 998 ºC) is shown in Table S1. Further discussion of the uncertainties regarding choice of V_A:V_M and potential limitations of the thermodynamic is given in the main text.

Table S1. Mixing ratio of selected species present in the input and output composition of HSC thermodynamic model. The input composition is discussed in the main text. H_2, CO and H_2S excluded as source species (replaced by Argon, noted by Ar^*) to prevent their re-equilibration (see text). For brevity, only species with > 10^{-13} mixing ratio output are shown.

Gas	Input (molar ratio)	Output (molar ratio)
H2O(g)	8.10E-01	8.10E-01
N2(g)	3.90E-02	3.90E-02
CO2(g)	9.04E-02	9.04E-02
SO2(g)	2.73E-02	2.69E-02
HCl(g)	1.32E-02	1.32E-02
O2(g)	1.05E-02	1.03E-02
Ar(g)	6.95E-03	6.95E-03
SO3(g)	0.00E+00	3.97E-04
SO(g)	0.00E+00	1.18E-09
NO(g)	0.00E+00	1.77E-05
HBr(g)	2.03E-05	1.54E-05
OH(g)	0.00E+00	1.00E-05
Cl(g)	0.00E+00	1.21E-05
Br(g)	0.00E+00	4.71E-06
Cl2(g)	0.00E+00	1.61E-06
I(g)	0.00E+00	3.55E-06
HOCl(g)	0.00E+00	3.34E-07
HI(g)	3.73E-06	2.56E-08
HF(g)	2.82E-03	2.83E-03
H(g)	0.00E+00	4.48E-10
H2SO4(g)	0.00E+00	1.42E-07
BrCl(g)	0.00E+00	1.78E-07
NO2(g)	0.00E+00	4.89E-08

ClO(g)	0.00E+00	3.88E-08
O(g)	0.00E+00	1.06E-08
HO2(g)	0.00E+00	2.28E-08
Br2(g)	0.00E+00	4.32E-09
HIO(g)	0.00E+00	6.92E-08
H2O2(g)	0.00E+00	3.02E-09
HNO2(g)	0.00E+00	1.02E-09
SOCl(g)	0.00E+00	2.72E-11
ICl(g)	0.00E+00	8.25E-08
BrO(g)	0.00E+00	6.56E-10
N2O(g)	0.00E+00	2.42E-10
NOCl(g)	0.00E+00	5.46E-10
HSO3Cl(g)	0.00E+00	3.03E-10
IBr(g)	0.00E+00	2.01E-09
IO(g)	0.00E+00	2.99E-10
NOBr(g)	0.00E+00	7.97E-12
HNO(g)	0.00E+00	2.75E-12
ClOO(g)	0.00E+00	4.54E-12
HNO3(g)	0.00E+00	8.20E-13
BrOO(g)	0.00E+00	1.08E-12
OClO(g)	0.00E+00	9.56E-13
O3(g)	0.00E+00	4.13E-13
I2(g)	0.00E+00	7.78E-11
ClO2(g)	0.00E+00	4.78E-13
SOCl2(g)	0.00E+00	2.07E-13
ClClO(g)	0.00E+00	1.61E-13
ClOCl(g)	0.00E+00	1.31E-13
NOI(g)	0.00E+00	3.62E-13
SOF(g)	0.00E+00	3.79E-11
IOO(g)	0.00E+00	3.08E-13
HSO3F(g)	0.00E+00	4.55E-10
ClOCl(g)	0.00E+00	1.31E-13
F(g)	0.00E+00	1.12E-11
ClF(g)	0.00E+00	5.92E-12
BrF(g)	0.00E+00	1.78E-12
IF(g)	0.00E+00	1.80E-11
NOF(g)	0.00E+00	2.53E-13
SO2ClF(g)	0.00E+00	5.68E-13

S2 Estimating the volcanic aerosol loading in Mt Etna's emission

Aerosol emissions from volcanoes are poorly constrained by observations to date. It is thus a challenge to quantify the volcanic aerosol surface area that is available to promote reactive halogen cycling. Few estimates of volcanic aerosol surface area loading exist, particularly in ash-poor plumes, and the available aerosol measurements are not always reported in the context of plume strength (e.g as indicated by a plume 'tracer' or quasi-tracer such as SO_2) For example, the study by Allen et al. (2006) reports in-situ aerosol measurements in conjunction with column abundances of SO_2, however these two methods sample different air masses thus cannot be directly compared. The *PlumeChem* modelling study of Figure 1 assumes both 'high' and 'medium' estimates for the aerosol surface area loading.

The 'high' estimate refers to a loading of $\sim 10^{-10}$ μm^2 molec.SO_2^{-1} equivalent to the $1.5 \cdot 10^{-5}$ cm^2 cm^{-3} $(\mu mol/mol\ SO_2)^{-1}$ estimate used in the model study of volcanic plume BrO chemistry by Roberts et al. (2009), which was derived from reported remote sensing measurements of particle surface area and SO_2 in Villarrica plume (Mather et al., 2004). However, it is possible that this estimate includes surface area from volcanic ash particles, and may not be representative of the Etna plume. Both ash and acid aerosols contribute to measured particle fluxes, however reactive uptake of HOBr (and $BrONO_2$) has to date only been quantified in acid aerosol and on ice (the chemistry is not known to occur on silica particles although the extent that halogen chemistry might occur on acid-coated ash particles is unknown).

The 'medium' estimate of volcanic aerosol refers to an aerosol surface area loading an order of magnitude lower ($\sim 10^{-11}$ μm^2 molec.SO_2^{-1}) than the 'high' estimate. This 'medium' aerosol loading (per molecule SO_2) estimate was also assumed in *PlumeChem* simulations of Redoubt volcano plume (Kelly et al., 2013) that found reasonably good agreement between the observed and modelled BrO-mediated plume ozone depletion. A further evaluation for Etna is attempted below using reported observational data, although remaining uncertainties in the volcanic aerosol emission are emphasized.

Spinetti and Buongiorno (2007) report airborne multispectral image observations, from which an aerosol effective radius of ~1 μm is derived for quiescent degassing conditions. Martin et al. (2008) and Allen et al. (2006) report in-situ measurements of Etna aerosol, although in the absence of concurrent in-situ measurements of SO_2 it is challenging to derive a value for the total particle surface area loading from these data. We supply the following rough calculation

of total aerosol surface area assuming particles of one radius size only. Based on reported sulphate:SO_2 molar ratio of 1:100 (Martin et al., 2008), and an estimated sulphate aerosol particle size of ~1 μm radius in the Etna Voragine crater emission (i.e. yielding individual particle volume of ~4.2 μm^3/particle), combined with an estimated total sulphate aerosol volume from E-AIM yielding ~$5 \cdot 10^{-5}$ cm^3 per m^3 in a plume containing 0.01 μmol/mol sulphate (280 K, 50% RH) i.e. for 1 μmol/mol (~10^{13} molec.cm^{-3}) SO_2 (see Roberts et al., 2014), a particle number concentration of 10^7 m^{-3} can be calculated, yielding a total particle surface area of ~10^{-11} μm^2 molec.SO_2. This estimate is consistent with our 'medium' aerosol loading.

Conversely, for the Etna plume, Watson and Oppenheimer (2000) report sun-photometer measurements of plume particles, from which a total particle mass flux of between 4.5 and 8.0 kg s^{-1} is derived. Assuming their end-member densities of sulphate ($1.67 \cdot 10^3$ kg/m^3) or water ($1 \cdot 10^3$ kg/m^3) yields volume fluxes of $(2.7\text{-}4.8) \cdot 10^{-3}$ $m^3 s^{-1}$ or $(4.5\text{-}8.0) \cdot 10^{-3}$ $m^3 s^{-1}$, which, using the reported mean effective radius, R_{eff} = 0.83 μm, yields a surface area flux range between 9700 and 28900 m^2/s. Concurrent SO_2 fluxes are not reported, but Watson and Oppenheimer's assumption of an Etna SO_2 flux of on the order of a thousand of tonnes per day (11.6 kg/s, note this is potentially underestimated by a factor of two, see main text) results in a surface area to SO_2 ratio of $(8.9 - 2.7) \cdot 10^{-10}$ μm^2 $molec^{-1}$ SO_2. This estimate is more consistent with the 'high' aerosol loading estimate. However a much wider range of surface area loadings (10^{-11} – 10^{-9} μm^2 $molec^{-1}$ SO_2) can be obtained if R_{eff} is allowed to vary (e.g. across the reported observations that show R_{eff} between 0.3 and 1.6 μm in their Figure 7b). A further issue is that, even though Watson and Oppenheimer (2006) report R_{eff} values from their sun-photometer measurements, the data actually indicate a substantial proportion of volcanic aerosol surface area is likely contributed by particles with radii beyond their reported measurement range (see their Figure 6b in particular) at either ≥ 5 μm or ≤ 0.1 μm respectively.

Ongoing work involving recently acquired in-situ aerosol measurements is attempting to refine these estimates of the volcanic surface area loading at Etna.

S3 The Pasquill-Gifford dispersion scheme.

The *PlumeChem* model dispersion scheme is based on a Gaussian plume with user-specified dispersion rates, thus can be constrained to available observations, for an example see Kelly et al. (2013). For these general investigations of the Etna plume a Pasquill-Gifford (PG) dispersion parameterisation (Pasquill, 1974, see e.g. Mudakavi, 2010 and references therein) was assumed, providing σ_h and σ_z dispersion parameters. These parameters are used directly to simulate Gaussian dispersion in multi-box mode, but for the single-box model mode, the plume was approximated as a single box with radius $\sqrt{2}\cdot\sigma_h$ and $\sqrt{2}\cdot\sigma_z$, i.e. plume area $2\cdot\pi\cdot\sigma_z\cdot\sigma_h$. The choice of PG dispersion case is a function of the atmospheric stability, thus depends on solar insolation wind-speed, as shown in Table S2, with the σ-parameters shown in Figures S1, and S2. It should be emphasized that the P-G dispersion schemes were principally developed for the dispersion of stack emissions in the atmospheric boundary layer above a flat surface rather than plume dispersion from a volcano summit, which emits into the free-troposphere for Etna (3.3 km asl). At Etna the wind-fields are rather complex and locally influenced by elevated surface topography of the mountain (Favalli et al., 2004). Nevertheless, the Pasquill-Gifford schemes provide a useful framework for preliminary studies investigating plume chemistry. To limit vertical dispersion under for the lower P-G cases, σz was capped at ≤ 1000 m.

Table S2 Pasquill-Gifford cases for varying wind-speed and solar insolation

Wind Speed m/s	Solar Insolation Strong	Solar Insolation Moderate	Solar Insolation Slight	Nigh Time Thin overcast or > ½ clouds	Night Time Conditions < 3/8 cloudiness
< 2	A	A-B	B	-	-
2-3	A-B	B	C	E	F
3-4	B	B-C	C	D	E
4-6	C	C-D	D	D	D
>6	C	D	D	D	D

Figure S1 Horizontal and vertical Pasquill-Gifford dispersion parameters.

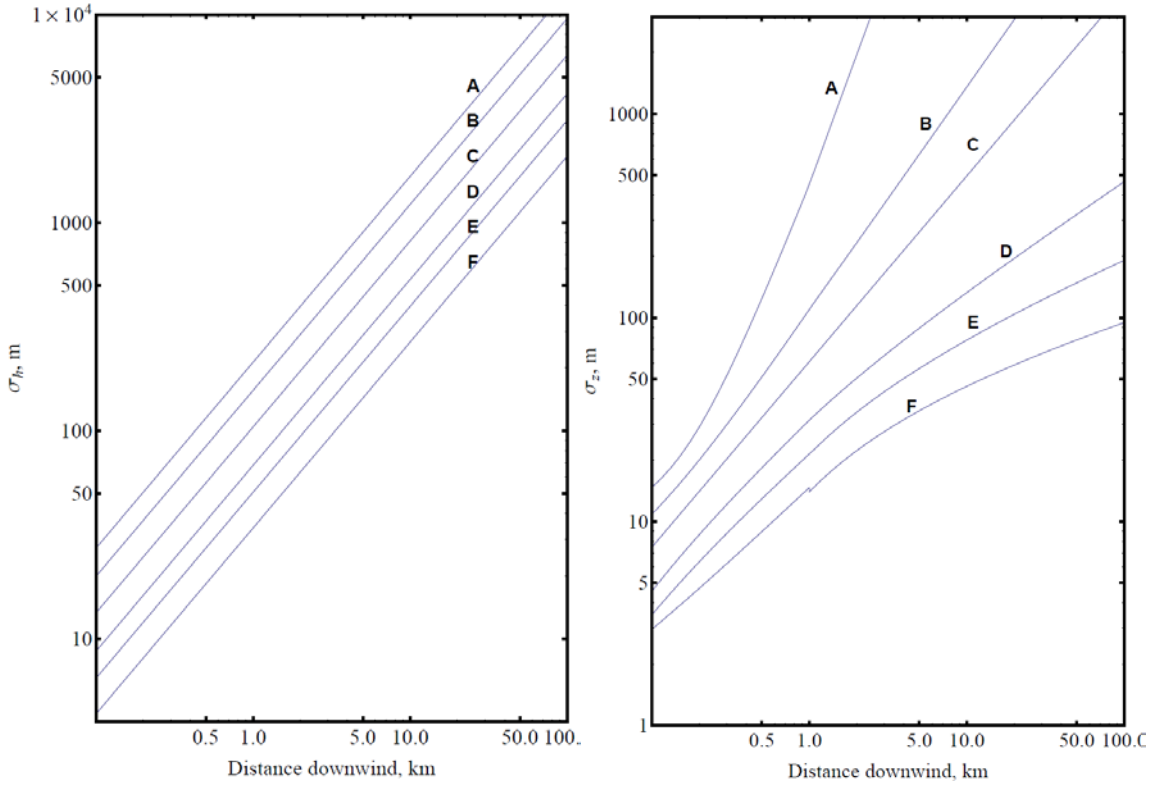

In the model sensitivity studies, PG case D (neutral atmosphere) was assumed for the base (daytime) model run at 10 m/s. Simulations under more unstable atmospheric conditions (faster dispersing plume) were also considered. Thus, cases C and D were investigated at 10 m/s, 15 m/s and 5 m/s and cases C and B at 3 m/s, according to Table S2. For each case, the Pasquill-Gifford dispersion parameters in the horizontal (cross-wind) and vertical, σ_h and σ_z were calculated as a function of distance downwind. Whilst actual plume-air mixing cannot be fully constrained from the available SO_2 column abundance, the base model run using PG dispersion case D (at 10 m/s windspeed and 10 kg/s SO_2 flux) exhibited general agreement to reported downwind SO_2 column data (see main text). Figure S2 illustrates the range in model SO_2 column abundances calculated for the runs with varying combinations of gas flux (10- 20 kg/s SO2), wind-speed (3, 5, 10, 15 m/s) and dispersion case (B, C, D) (see the main text Figure 6 for the colour scale labelling). Some of these alternative model simulations also show agreement to the reported data whilst others somewhat over-predict downwind SO_2.

Figure S2. Downwind SO_2 columns predicted for the range of assumed dispersion rate (B, C, D), wind-speed (3,5,10,15 m/s) and gas flux (10, 20 kg/s) in the *PlumeChem* model, compared to data reported by Bobrowski et al. (2007a) and Oppenheimer et al. (2006), black disks and gray squares respectively.

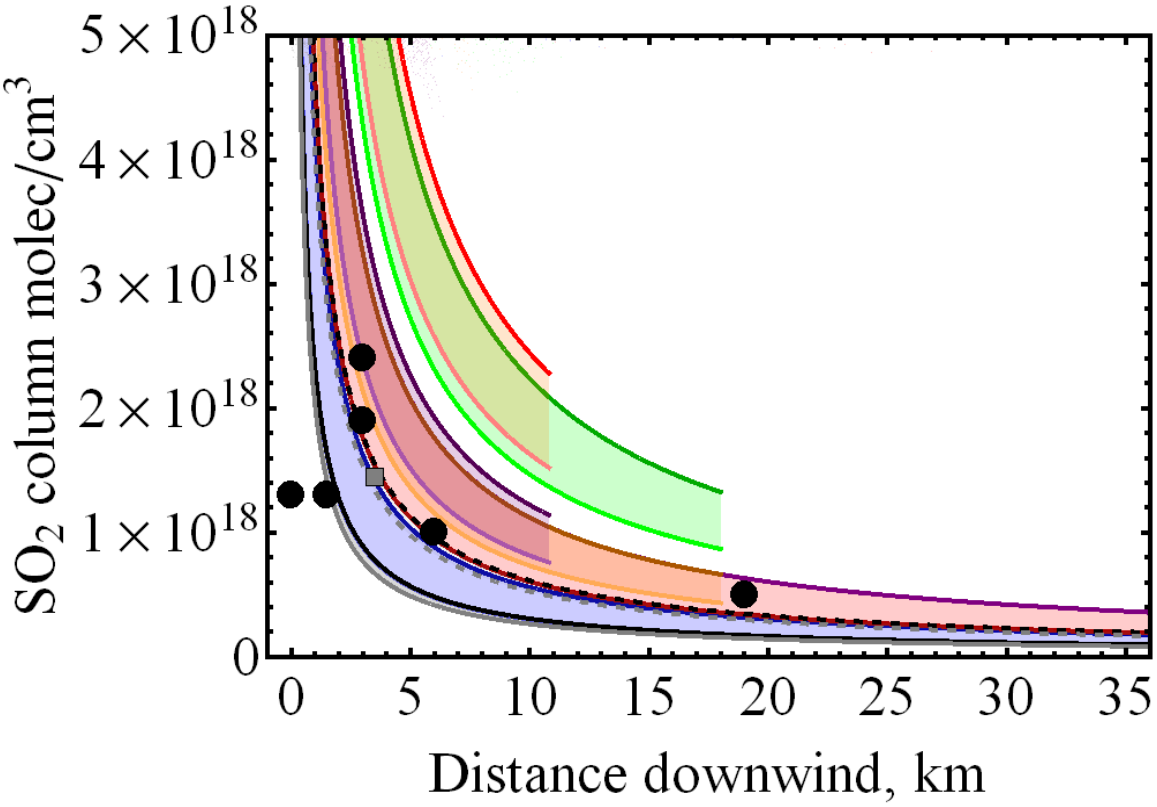

S4 Background atmospheric composition

The *PlumeChem* model results presented for Etna assumed a relatively polluted background atmosphere. The chemical composition of the background atmosphere was calculated separately to the plume, in a box model that includes gas-phase and photolytic HO_x, NO_x, O_x and methane oxidation chemistry, after a ~10-day spin-up period. The model simulates diurnal photochemistry, although for this specific study most species in the background atmospheric composition do not substantially change abundance over the 1-3 hr simulations of Etna plume (starting ~ midday on 19 August 2004). However the background box model does not simulate heterogeneous-phase reactions or gas-aerosol partitioning. This presents a limitation to the model e.g. for HNO_3 which will enter the particle phase, although this species is likely re-volatilised upon entrainment of background air into strong and highly acidic plume environments. Table S2 presents background atmospheric composition at the

start of the plume model run. Note total HNO_3 abundance is somewhat high (very polluted condition), which will be corrected in future model runs. Nevertheless tests (not shown) found *PlumeChem* plume model runs yield near identical results for the major features of the volcano plume BrO chemistry when the background HNO_3 is reduced by a factor of 10.

Table S2. Background atmospheric composition at the start of the plume model run. Species such as $O(^1D)$ and $O(^3P)$ were calculated in steady-state (with respect to ozone).

Species	Mixing Ratio in background air at plume model start time (mol/mol)
O_3	$6.4 \cdot 10^{-8}$
NO	$5.0 \cdot 10^{-11}$
NO_2	$1.1 \cdot 10^{-10}$
NO_3	$5.0 \cdot 10^{-14}$
N_2O_5	$1.4 \cdot 10^{-14}$
HNO_3	$5.8 \cdot 10^{-9}$
HONO	$2.0 \cdot 10^{-12}$
OH	$6.9 \cdot 10^{-13}$
HO_2	$3.0 \cdot 10^{-11}$
H_2O_2	$2.0 \cdot 10^{-9}$
CO	$1.5 \cdot 10^{-7}$
CH_3O_2	$1.0 \cdot 10^{-11}$
CH_3OH	$6.0 \cdot 10^{-12}$
CH_4	$1.7 \cdot 10^{-6}$
HCHO	$5.5 \cdot 10^{-10}$

References

Allen A. G., Mather T. A., McGonigle A. J. S. , Aiuppa A., Delmelle P., Davison B., Bobrowski N., Oppenheimer C. , Pyle D.M., Inguaggiato S., Sources, size distribution, and downwind grounding of aerosols from Mount Etna, Journal of Geophysical Research, 111, D10302, doi:10.1029/2005JD006015, 2006.

Bobrowski, N., von Glasow, R., Aiuppa, A., Inguaggiato, S., Louban, I., Ibrahim, O. W. and Platt, U.: Reactive halogen chemistry in volcanic plumes, J. Geophys. Res., 112, D06311, doi;101029/2006JD007206, 2007a.

Favalli, M. Mazzarini F., Teresa Pareschi M. Boschi E., Role of local wind circulation in plume monitoring at Mt. Etna volcano (Sicily): Insights from a mesoscale numerical model, Geophysical Research Letters, 31, L09105, doi:10.1029/2003GL019281, 2004.

Kelly P.J., Kern C., Roberts T.J., Lopez T., Werner C., and Aiuppa A.: Rapid chemical evolution of tropospheric volcanic emissions from Redoubt Volcano, Alaska, based on observations of ozone and halogen-containing gases, Journal of Volcanology and Geothermal Research, Journal of Volcanology and Geothermal Research, 259, 317–333, 2013.

Mather, T.A., Tsanev, V.I., Pyle, D.M., McGonigle, A.J.S, Oppenheimer, C., Allen, A.G., 2004. Characterization and evolution of tropspheric plumes from Lascar andVillarrica volcanoes, Chile. Journal of Geophysical Research, 109, D21303. doi:10.1029/2004JD004934, 2004.

Martin, R. S., Mather, T. A., Pyle, D. M., Power, M. Allen, A. G., Aiuppa, A., Horwell, C. J. and Ward E. P. W.: Composition-resolved size distributions of volcanic aerosols in the Mt. Etna plumes, Journal of Geophysical Research, 113, D17211, doi:10.1029/2007JD009648, 2008.

Mudakavi, J. R. Principles and practices of Air Pollution Control and analysis. IK International Pvt Ltd, 2010.

Oppenheimer, C., Tsanev, V. I., Braban, C. F., Cox, R. A., Adams, J. W., Aiuppa, A., Bobrowski, N., Delmelle, P., Barclay, J. and McGonigle, A. J. S.: BrO formation in volcanic plumes. Geochim. Cosmochim. Ac., 70, 2935-2941, 2006.

Pasquill, F., 1974. Atmospheric Diffusion; the dispersion of windborne material from industrial and other sources. Ellis Horwood, Chichester.

Roberts, T. J., Braban, C. F., Martin, R. S., Oppenheimer, C., Adams, J. W., Cox, R. A., Jones R. L. and Griffiths., P. T, Modelling reactive halogen formation and ozone depletion in volcanic plumes. Chem. Geol., 263,151-163, 2009.

Roberts T. J., Jourdain L., Griffiths P. T., Pirre M., Re-evaluating the reactive uptake of HOBr in the troposphere with implications for the marine boundary layer and volcanic plumes, in review, ACPD, 2014.

Spinetti and Buongiorno, Volcanic aerosol optical characteristics of Mt. Etna tropospheric plume retrieved by means of airborne multispectral images, Journal of Atmospheric and Solar-Terrestrial Physics, 69, 981–994, 2007.

Watson and Oppenheimer, Particle size distributions of Mount Etna's aerosol plume constrained by Sun photometry, Journal of Geophysical research, 105, D8, 823-982, 2000.